Enhancement of the power conversion efficiency of polymer solar cells by functionalized single-walled carbon nanotubes decorated with CdSe/ZnS core-shell colloidal quantum dots

9 AUTHORS, INCLUDING:

Fan Zou
Shanghai Institute of Optics and Fine Mech…
4 PUBLICATIONS **11** CITATIONS

SEE PROFILE

Jinquan Wei
Tsinghua University
190 PUBLICATIONS **5,266** CITATIONS

SEE PROFILE

Bingsuo Zou
Beijing Institute of Technology
278 PUBLICATIONS **7,574** CITATIONS

SEE PROFILE

Enhancement of the power conversion efficiency of polymer solar cells by functionalized single-walled carbon nanotubes decorated with CdSe/ZnS core–shell colloidal quantum dots

Ting Ni · Jingying Yan · Yurong Jiang ·
Fan Zou · Li Zhang · Dan Yang · Jinquan Wei ·
Shengyi Yang · Bingsuo Zou

Abstract In this paper, we demonstrated an enhanced performance of polymer solar cells by incorporating functionalized single-walled carbon nanotubes (SWCNTs) decorated with CdSe/ZnS core–shell colloidal quantum dots (CQDs) into copolymers of poly(3-hexylthiophene) (P3HT) and [6,6]-phenyl-C_{61}-butyric acid methyl ester (PCBM) as active layer. Short-circuit current density and power conversion efficiency of the ITO/PEDOT:PSS/ P3HT:PCBM:(CdSe/ZnS-SWCNTs)/Al solar cells can be enhanced by more than 31 and 23 %, respectively, as compared with the control device ITO/PEDOT:PSS/ P3HT:PCBM/Al. This enhancement is due to the high electron-transporting ability of SWCNTs and the increased absorption of CdSe/ZnS CQD in visible region. It shows an applicable way to improve the efficiency of polymer solar cells by incorporating suitable quantity of CQDs-decorated SWCNTs with suitable kinds of CQDs and suitable acid treatment to the SWCNTs.

T. Ni · Y. Jiang · F. Zou
Beijing Key Lab of Nanophotonics and Ultrafine Optoelectronic Systems, School of Optoelectronics, Beijing Institute of Technology, Beijing 100081, People's Republic of China

J. Yan · D. Yang · S. Yang (✉) · B. Zou
Beijing Key Lab of Nanophotonics and Ultrafine Optoelectronic Systems, School of Physics, Beijing Institute of Technology, Beijing 100081, People's Republic of China
e-mail: syyang@bit.edu.cn

L. Zhang
Beijing Key Lab of Nanophotonics and Ultrafine Optoelectronic Systems, School of Materials Science and Engineering, Beijing Institute of Technology, Beijing 100081, People's Republic of China

J. Wei
Key Lab for Advanced Materials Processing Technology of Education Ministry, School of Materials Science and Engineering, Tsinghua University, Beijing 100084, People's Republic of China

Introduction

Recently, organic photovoltaics have attracted much interest due to their strong prospective to realize low cost power generation, improved scalability, and opportunity for lightweight, flexible devices [1]. To date, most of polymeric thin film nanocomposite devices are based on the bulk heterojunction (BHJ) concept [2]. The principle of the BHJ is that a donor and an acceptor material are blended together in nanoscale morphology to form a network configuration improving the separate probability of excitons. This structure is formed during spin-coating from a common solvent. Usually, the electron donor is a conducting polymer, such as poly(3-hexylthiophene) (P3HT) or poly(3-octylthiophene) (P3OT), which has high absorption coefficient in the visible region of the solar spectra and a high mobility for photogenerated holes, and the electron acceptor is usually a fullerene derivative, such as [6,6]-phenyl-C_{61}-butyric acid methyl ester (PCBM) [2, 3].

Particularly, a highly efficient polymer-fullerene BHJ solar cells with a certified efficiency of 9.2 % were reported recently [4], using an inverted structure which simultaneously offers ohmic contact for photogenerated charge-carrier collection and allows optimum photon harvest in the device. Compared with silicon-based photovoltaics, polymer solar cells suffer from insufficient light absorption due to the thin active layer restricted by the short exciton diffusion length ($\sim$10 nm) of the polymer and low carrier mobilities [2, 5]. Hence, promising approaches to improve the absorption of polymer solar cells are to blend with narrow

band-gap colloidal quantum dots (CQDs) or to embed metallic nanoparticles (NPs) into active layer. Narrow band-gap CQDs can create multiple excitons when a single photon having energy much higher than its bandgap is absorbed by the CQDs. At the same time, by changing the size of the CQDs one can realize tuning its absorption spectra [6–9]. However, the ligands of the CQDs are inert insulators and they usually block the charge carriers transport in the active layer, thus the carrier mobilities are very low. On the other hand, if one directly blends non-ligand-exchanged CQDs into the active layer, it may have negative effect on the quality of the active layer surface because of the agglomerating of CQDs. As reported by Zhou et al. [10], the power conversion efficiency (PCE) of hybrid solar cell based on non-ligand-exchanged CdSe quantum dots and P3HT is only 2 %. In order to reduce the surface flaws of CQDs, core/shell structure has been used to produce CQDs, implying CQD is usually capped with a smooth shell. As Dixit et al. [6] reported, the PCE of CdSe/ZnS CQDs-based hybrid solar cell ITO/PEDOT:PSS/P3HT:(CdSe/ZnS)/LiF/Al reached 5.1 % in which the CdSe/ZnS core/shell CQDs were used as electron acceptor and they diffuse into P3HT to form BHJ after thermal annealing. Therefore, reducing the surface flaws of CQDs has positive effects on the performance of the devices. Although incorporating CQDs can improve the performance of the polymer solar cells in the fields of absorption and utilization of the incident light, the ligands and surface flaws of CQDs will be barriers for further improvement. An available method is to take advantage of the fast charge carriers transport ability of SWCNTs to improve the charge carriers transfer from CQDs to polymers, and finally to electrodes. Landi et al. [1] reported that the PCE of hybrid solar cell based on CdSe-aminoethanethiol-SWCNT and P3OT is below 1 % under illumination of 1 Sun AM0, but the PCE of hybrid solar cell based on the PbS CQD-MWCNT nanocomposite increases to 3.03 %, and it has been improved by 17.9 % as compared with solar cells without incorporating the nanocomposites [11]. In their experiments, PbS CQD-MWCNT nanocomposites were linked up by weak intermolecular forces between oleyl amine (OLA)-capped CQDs and OLA-capped MWCNTs. Kim and co-workers [12] reported that the PCE of polymer solar cell ITO/PEDOT:PSS/P3HT:ICBA:CQD-MWCNT/ TiO$_x$/Al, in which indium phosphite QDs/N-doped CNT hybrid nanomaterials as active layer, attains to 6.11 %. All the results mentioned above confirm the promise of CQD-CNT nanoarchitecture in increasing the efficiency of hybrid solar cells. However, what is the best way to acid-treat the SWCNTs? And how much the PCE can be improved by this kind of incorporating CdZe/ZnS-SWCNTs nanocomposites into P3HT:PCBM copolymers? Especially, is it possible to improve the PCE of polymer solar cells with CQDs emission in visible region?

In this paper, we firstly prepared functionalized SWCNTs by an easy acid treatment and then to decorate them with CdSe/ZnS core–shell CQDs, and then blended this as-synthesized CdSe/ZnS-SWCNTs nanocomposites into P3HT:PCBM as active layer, and we found that the efficiency of hybrid solar cell ITO/PEDOT:PSS/ P3HT:PCBM:(CdSe/ZnS-SWCNT)/Al has been improved by 23.3 %, i.e., from 2.75 to 3.39 %, as compared to the control device ITO/PEDOT:PSS/P3HT:PCBM/Al in which the weight ratio of P3HT to PCBM is 1:0.8. From our experimental data, we believe that the PCE of polymer solar cells can be further enhanced by incorporating such a kind of the as-synthesized CQDs-decorated SWCNTs as active layer, especially for its short-circuit current density.

Experimental

Optimization of acid-treated SWCNTs

Usually, the untreated SWCNTs contain some metallic impurities and this part of metallic impurities can be removed by the acid treatment [11, 13]. At the same time, acid treatment can make SWCNTs be coated with carboxyl (–COOH), in this way, one can improve the dispersivity of SWCNTs in ortho-dichlorobenzene (ODCB).

As we know, much higher extent of acid treatment, the conductivity of SWCNTs will get lower, sequentially it will decrease the mobilities of charge carriers in block polymers. Therefore, the extent of acid treatment on SWCNTs is crucial not only for synthesizing CdSe/ZnS-SWCNT, but also for increasing the short-circuit current of the solar cells. In order to choose a suitable way to functionalize SWCNT, in our experiments we tried three methods of acid treatment: (1) To disperse SWCNTs in the dilute nitric acid (HNO$_3$, 3 M), sonicating for 4 h at room temperature [11]. (2) To disperse SWCNTs in the mixture of concentrated hydrochloric acid (HCl, 12 M) and H$_2$O$_2$ with a volume ratio of 1:3 [14, 15] after SWCNTs were soaked in the hydrogen peroxide (H$_2$O$_2$) for 3–5 days. and (3) To disperse SWCNTs in the mixture of sulfuric acid (98 % H$_2$SO$_4$) and nitric acid (98 % HNO$_3$) in a volume ratio of 3:1, stirring for 4 h at room temperature [16]. All above acid-treated SWCNTs were obtained after washing with deionized water until the pH value was close to 7 and then they were dispersed in ODCB.

Decorating SWCNT with CdSe/ZnS CQDs

In our experiments, the CdSe/ZnS core–shell CQDs were bought from Wuhan Jiayuan Quantum Dots Co. Ltd, China. We used CdSe/ZnS core–shell CQDs to decorate SWCNT because such a kind of core/shell CQDs can reduce its surface flaws. CdSe/ZnS core–shell CQDs were

capped with OLA which has one amino (–NH$_2$) and it can act as the bridge between SWCNT and CQDs. According to the recent literatures [11, 16, 17], we used a simple way to realize the linkage between SWCNTs and CdSe/ZnS CQDs. The carboxyls on the surfaces of SWCNTs can react with amino attached on CQDs by weak bond energy, although this reaction happens between weak acid and weak base. As shown in Fig. 1, CdSe/ZnS CQDs decorate onto SWCNTs by hydrogen bond. Firstly, the acid-treated SWCNTs were completely dispersed in

ODCB, and then OLA-capped CdSe/ZnS CQDs were mixed with them (40:1 by weight) by sonication for 15 min until the solution is optically transparent [11, 18–20]. Then, purification via centrifugation (6000 rpm, 5 min) was made to discard the supernatant and to remove those unattached free CQDs. Although the QD density onto SWCNTs is not easy to evaluate because most of unattached free CQDs have been removed from the solution, we finally obtained the CdSe/ZnS-SWCNT nanocomposites.

Fig. 1 The process of CdSe/ZnS CQDs decorate onto acid-treated SWCNTs by hydrogen bond

CdSe/ZnS CQDs capped with OLA

Acid-treated SWCNT

CdSe/ZnS CQDs decorated onto SWCNTs by hydrogen bond.
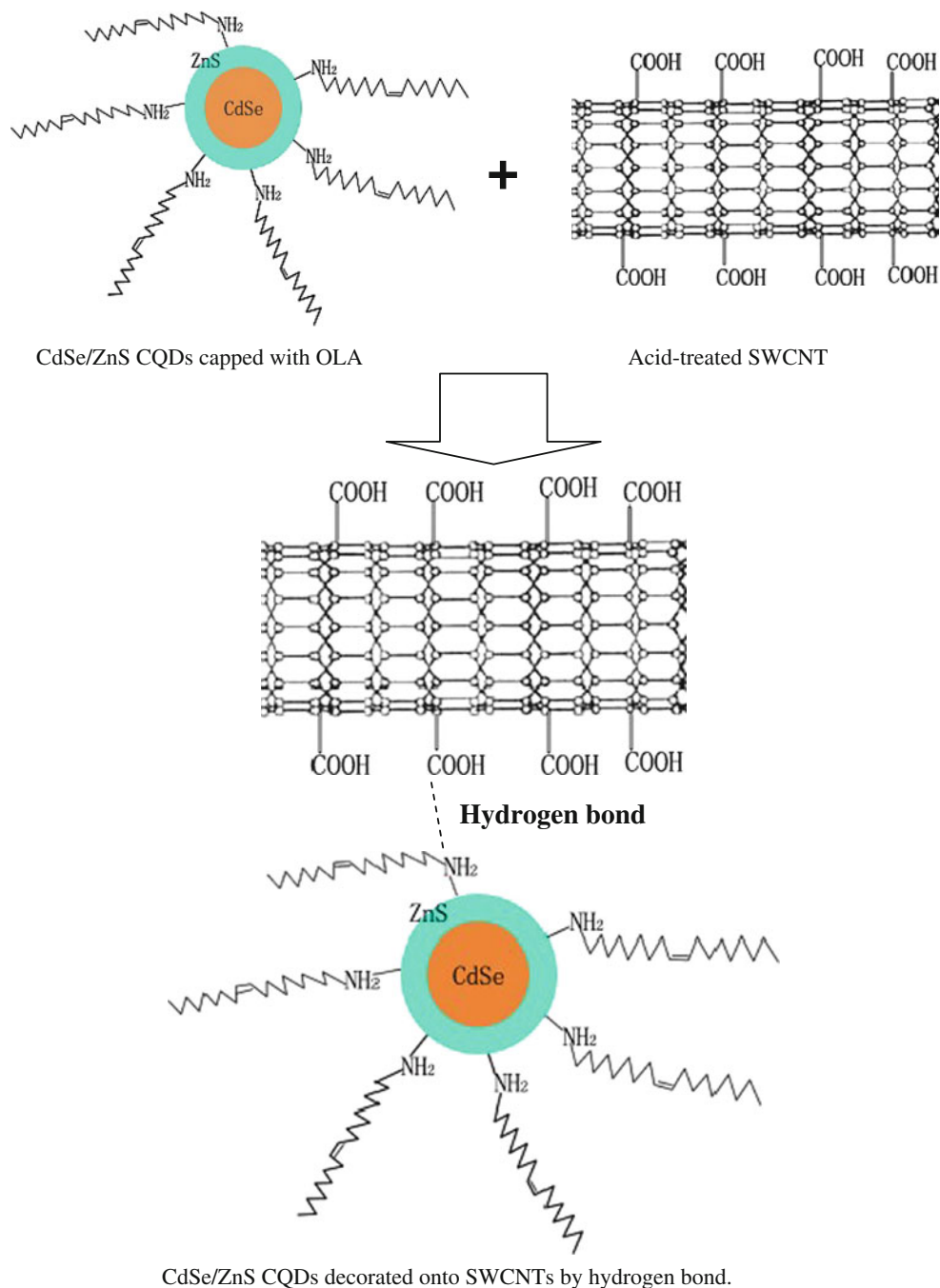
Device fabrication

The BHJ devices were fabricated in a traditional sandwich structure with an indium-tin oxide (ITO) as positive electrode and Al as negative electrode. Firstly, patterned ITO glass was cleaned and treated in an oxygen plasma chamber for 3 min, then PEDOT:PSS was spin-coated at 2000 rpm for 60 s on the ITO electrode. Subsequently, the PEDOT:PSS film was baked at 130 °C for 30 min in air. A blended solution of P3HT and PCBM (1:0.8 by weight, i.e., 20 and 16 mg/mL, respectively) in ODCB was stirred overnight at room temperature, and then it was spin-coated on top of PEDOT:PSS layer at 800 rpm for 60 s in a nitrogen glove box. This choice of spinning rate and duration time reproducibly gives a solid active film with a thickness of around 150 nm. We put the glass substrate inside a covered Petri dish dwelling in the glove box until the characteristic color of the film changes from a light yellow to a dark purple till the film solidified [2, 21]. For the active layer of hybridized polymer solar cells, according to the reports [11, 22, 23], the concentration of SWCNTs was controlled around 0.1 mg/mL. Therefore, we used 4 mg OLA-capped CdSe/ZnS CQDs to decorate with SWCNTs, and then to blend solution of CdSe/ZnS-SWCNT nanocomposites and P3HT:PCBM into ODCB. The active layer of hybrid polymer solar cells was produced by the same steps. After the appropriate dwelling procedures, the negative electrode of Al ($\sim$150 nm) was thermally evaporated on the active layer with a shadow mask in a base pressure of 3×10^{-4} Pa. Finally, devices were annealed in the glove box at 150 °C for 20 min. The device active area was $\sim$9 mm^2. All the measurements were carried out at room temperature in air.

Results and discussion

Figure 2 shows Raman spectra of different SWCNTs under 532 nm laser, showing the extent of acid treatment by above three methods. As compared with untreated SWCNTs, the intensity ratio of peak D to peak G (defined by $R = I_D/I_G$) of acid-treated SWCNTs changes with the extent of acid treatment. R reaches 0.682 for the SWCNTs treated by HNO$_3$:H$_2$SO$_4$ and it is the highest value of intensity ratio for these three cases. On the other hand, R reaches 0.247 for the SWCNTs treated by HCl:H$_2$O$_2$ and it is the lowest value of intensity ratio for those treated SWCNTs.

As we know, R reflects the order and the purity of SWCNTs [13, 24–26]. Acid treatment will make SWCNTs be coated with carboxyls by breaking the chemical bonds on the tube wall [16], resulting in a decrease of both the order and the purity of SWCNTs [24–26]. Therefore, we adopt the second method to deal with SWCNTs and then to
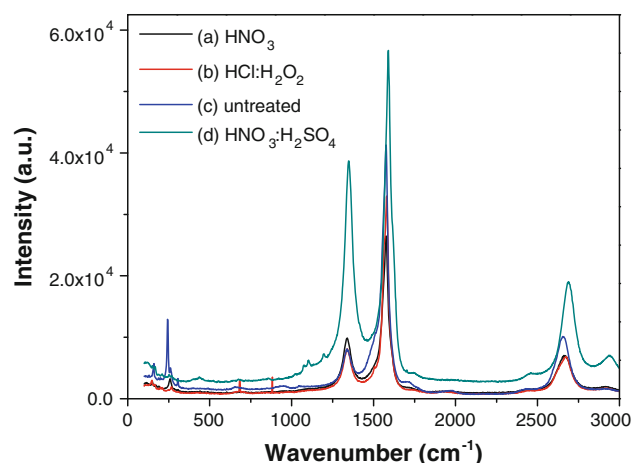

Fig. 2 Raman spectra of different SWCNTs: *a* treated by 3 M HNO$_3$; *b* treated by 12 M HCl:H$_2$O$_2$; *c* untreated SWCNTs; *d* treated by HNO$_3$:H$_2$SO$_4$
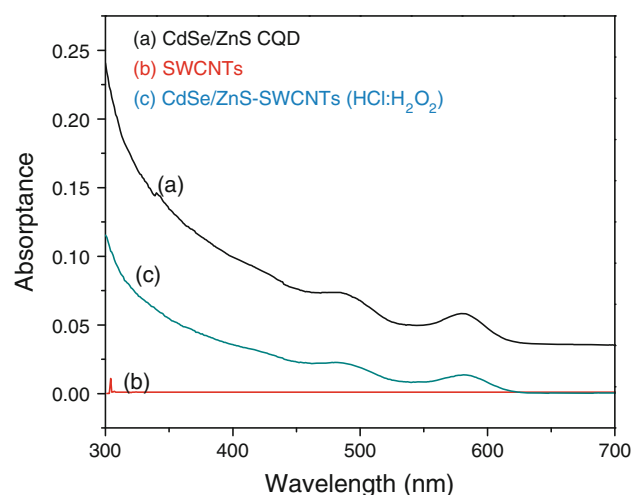

Fig. 3 Absorption spectra of materials used in our experiments. *a* CdSe/ZnS CQDs; *b* SWCNTs; *c* CdSe/ZnS-SWCNT in which SWCNT was treated with HCl:H$_2$O$_2$

coat SWCNTs with carboxyls, in this way, and to preserve the conductivity of SWCNTs.

Figure 3 shows the absorption spectra of CdSe/ZnS CQDs, primitive SWCNTs, and the as-synthesized CdSe/ZnS-SWCNT nanoarchitecture in which SWCNTs were treated by concentrated H$_2$O$_2$:HCl. Obviously, from here one can see that the CdSe/ZnS-SWCNT has two absorption peaks, and they originate from CdSe/ZnS CQDs. This could be further confirmed by the fact that purified CdSe/ZnS-SWCNT nanoarchitectures were present, while the unattached CQDs were completely removed by repeated centrifugation. Therefore, these absorption peaks of CdSe/ZnS-SWCNT nanocomposites could be from CQDs which situated on SWCNTs surfaces. Therefore, the absorption
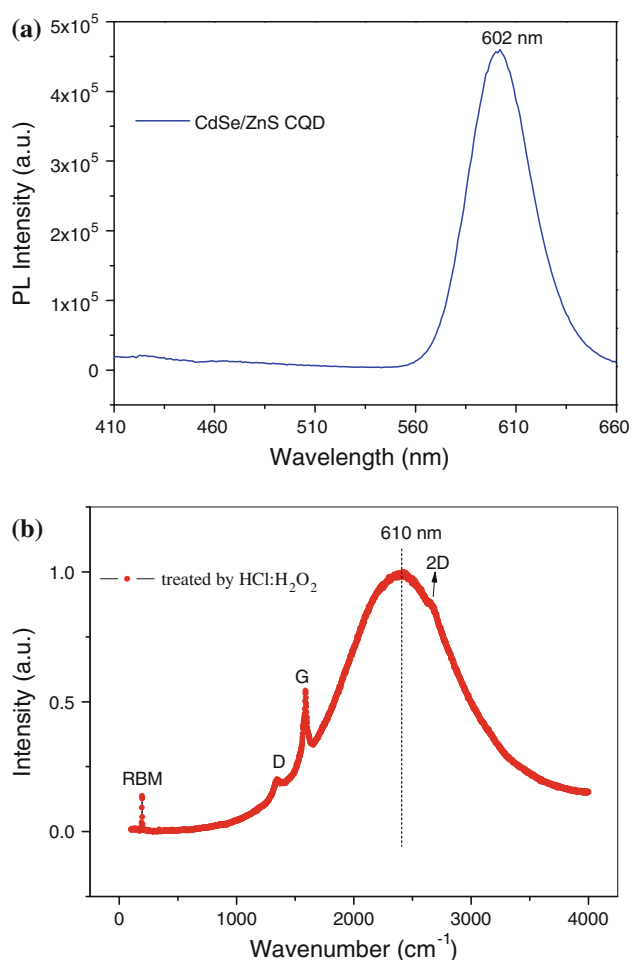
Fig. 5 TEM micrographs for the CdSe/ZnS-SWCNT nanocomposites

Fig. 4 a Photoluminescence spectrum of CdSe/ZnS CQD. **b** Raman spectra of CdSe/ZnS-SWCNT treated by concentrated HCl:H$_2$O$_2$, under excitation of 532 nm laser. Here, one can see that the characteristic peaks of SWCNTs, i.e., RBM peak at 193.6 cm^{-1}, D peak at 1344.8 cm^{-1}, G peak at 1588.3 cm^{-1}, and 2D peak at 2677.4 cm^{-1}. The PL of CdSe/ZnS-SWCNT peaks at 2405 cm^{-1} and it corresponds to peak wavelength at 610 nm

Fig. 6 J–V curves for photovoltaic cells *a* ITO/PEDOT:PSS/ P3HT:PCBM/Al and *b* ITO/PEDOT:PSS/P3HT:PCBM:(CdSe/ZnS-SWCNT)/Al in which SWCNTs were treated by concentrated HCl:H$_2$O$_2$

spectra show us that CdSe/ZnS CQDs have really been decorated to the SWCNTs surfaces.

Figure 4a shows the PL spectra of CdSe/ZnS CQD, showing it peaks at 602 nm. Figure 4b shows the Raman spectra of CdSe/ZnS-SWCNT treated by concentrated HCl:H$_2$O$_2$ under excitation wavelength of 532 nm laser. The characteristic peaks of SWCNTs, such as RBM peak, D peak, G peak and 2D peak, and the PL peak of CdSe/ZnS-SWCNT are shown here, which confirm that CdSe/ZnS CQDs have really been attached to the surfaces of SWCNT. It is worthy to note that the PL peak of CdSe/ZnS-SWCNT treated by concentrated HCl:H$_2$O$_2$ redshifts from 602 to 610 nm, and it could be due to the following reasons: (1) The distance between CQD and SWCNT decreased, and it leads to the enhancement of ion–dipole interaction so that the stokes shift increases and PL peak of
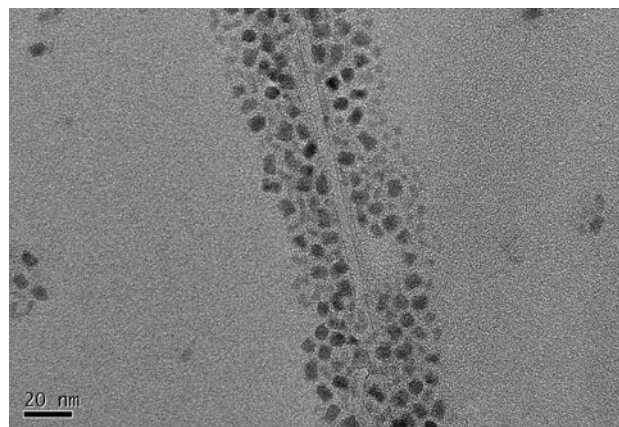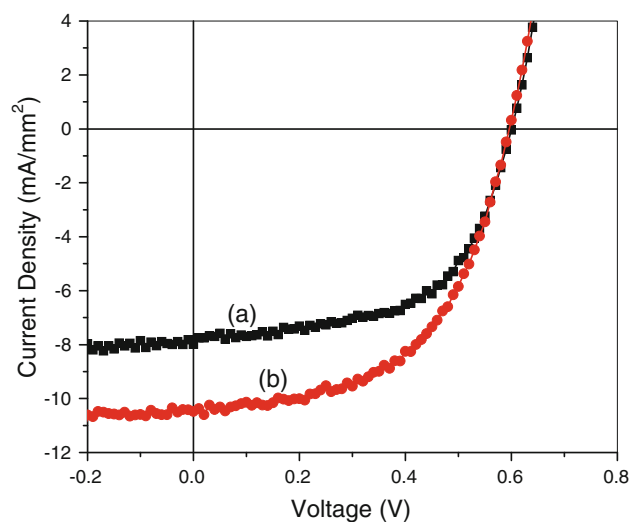
CdSe/ZnS CQD has a slight redshift [27, 28]; (2) the CdSe/ZnS-SWCNT nanocomposites exhibited PL quenching of CdSe/ZnS CQDs. The high energy electrons produced by PL excitation are easy to transport by SWCNT which results in a decreasing of high energy electrons so that the PL peak of CdSe/ZnS CQD has a slight redshift [25, 29–31]. The TEM micrographs for the CdSe/ZnS-SWCNT are shown in Fig. 5, in which the morphologies of the nanocomposite can be identified clearly.

Therefore, based on the experimental data on above three kinds of acid-treated SWCNTs, we fabricated two kinds of photovoltaic devices: device **A** (ITO/PEDOT:PSS/P3HT:PCBM/Al) and device **B** (ITO/PEDOT:PSS/P3HT:PCBM:(CdSe/ZnS-SWCNT)/Al) in which SWCNTs were treated by concentrated HCl:H$_2$O$_2$. The J–V curves of these

Table 1 Performance of solar cells **A** and **B**. All the PCE data shown here are corrected for spectral mismatch between the sun simulator and AM 1.5 spectra

Device	V_{OC} (V)	J_{SC} (mA/cm^2)	FF (%)	PCE (%)
A	0.6	7.99	58.9	2.75
B	0.6	10.48	53.9	3.39

photovoltaic devices are shown in Fig. 6, and the cell performance for devices **A** and **B** is summarized in Table 1. From Fig. 6 and Table 1, one can see that the incorporation of CdSe/ZnS-SWCNT nanocomposites in P3HT:PCBM as active layer can really increase the short-circuit current (J_{SC}) of the solar cell by about 31.2 %, i.e., from 7.99 to 10.48 mA/cm^2. The reason for this improvement is that CdSe/ZnS-SWCNT nanocomposites can accelerate the transport of electron in the blended polymers and enhance the light absorption in visible region, in this way, to produce more charge carriers than the traditional devices. In the polymers blended with CdSe/ZnS-SWCNTs, bigger surface area of BHJ has been built to promote the separation of excitons, and also it is helpful to increase the short-circuit current of solar cells.

Although the current has been enhanced after blending CdSe/ZnS-SWCNT in the active layer, the fill factor (FF) decreased by 9.28 %. This phenomenon shows that SWCNTs may have negative effect on the film smoothness and it results in a number of traps in the active layer.

The open-circuit voltage (V_{OC}) mainly depends on the difference of energy level between electron donor and electron acceptor. Because the proportion of CdSe/ZnS-SWCNT in active layer is low, hence V_{OC} mainly depends on P3HT:PCBM. Therefore, V_{OC} is kept at around 0.6 V for these two types of solar cells. More importantly, the PCE of the device **B** has been improved by 23.3 % after incorporating CdSe/ZnS-SWCNT in P3HT:PCBM as compared with that of device **A**. The PCE can be further improved if one use near infrared CQDs and firstly to take ligand-exchange CQDs with shorter ligands and then decorate it with SWCNTs, as well as another buffer layer was inserted in the devices, and all these experiments are under investigation.

Conclusions

In conclusion, we have demonstrated a 23.3 % enhancement in efficiency of photovoltaic devices by incorporating CdSe/ZnS-SWCNT nanocomposites into BHJ copolymers P3HT:PCBM as active layer. Our experimental data confirm that the PCE of polymer solar cells can be improved by incorporating CQDs in visible region, and CdSe/ZnS-

SWCNT nanocomposites have a positive effect on the solar cell performance, for our case the short-circuit current density has been improved by more than 31.2 %. It provides a promising way to improve polymer solar cells by incorporating suitable quantity of CQDs-decorated SWCNTs into the polymers with suitable kind of CQDs with strong light absorption and suitable acid treatment to the SWCNTs. There might be still some space to improve the efficiency of polymer solar cells after optimizing device fabrication parameters.

References

1. Landi BJ, Castro SL, Ruf HJ, Evans CM, Bailey SG, Raffaelle RP (2005) CdSe quantum dot-single wall carbon nanotube complexes for polymeric solar cells. Sol Energy Mater Sol Cells 87:733–746
2. Chang LL, Lademann HWA, Bonekamp JB, Meerholz K, Moulé AJ (2011) Effect of trace solvent on the morphology of P3HT:PCBM bulk heterojunction solar cells. Adv Funct Mater 21:1779–1787
3. Li G, Shrotriya V, Huang J, Yao Y, Moriarty T, Emery K, Yang Y (2005) High-efficiency solution processable polymer photovoltaic cells by self-organization of polymer blends. Nat Mater 4:864–868
4. He ZC, Zhong CM, Su SJ, Xu M, Wu HB, Cao Y (2012) Enhanced power-conversion efficiency in polymer solar cells using an inverted device structure. Nat Photonics 6:591–595
5. Markov DE, Amsterdam E, Blom PWM, Sieval AB, Hummelen JC (2005) Accurate measurement of the exciton diffusion length in a conjugated polymer using a heterostructure with a side-chain cross-linked fullerene layer. J Phys Chem A 109:5266–5274
6. Dixit SK, Madan S, Madhwal D, Kumar J, Singh I, Bhatia CS, Bhatnagar PK, Mathur PC (2012) Bulk heterojunction formation with induced concentration gradient from a bilayer structure of P3HT:CdSe/ZnS quantum dots using inter-diffusion process for developing high efficiency solar cell. Org Electron 13:710–714
7. Landsber PT, Nussbaumer H, Willeke G (1993) Band–band impact ionisation and solar cell efficiency. J Appl Phys 74:1451–1452
8. Wang LD, Zhao DX, Su ZS, Li BH, Zhang ZZ, Shen DZ (2011) Enhanced efficiency of polymer/ZnO nanorods hybrid solar cell sensitized by CdS quantum dots. J Electrochem Soc 158:H804–H807
9. Kolodinski S, Werner JH, Wittchen T, Queisser HJ (1993) Quantum efficiencies exceeding unity due to impact ionization in silicon solar cells. Appl Phys Lett 63:2405–2407
10. Zhou YF, Riehle FS, Yuan Y, Schleiermacher HF, Niggemann M, Gerald AU, Michael K (2010) Improved efficiency of hybrid solar cells based on non-ligand-exchanged CdSe quantum dots and poly(3-hexylthiophene). Appl Phys Lett 96:013304
11. Wang DF, Baral JK, Zhao HG, Gonfa BA, Truong VV, Khakani MAE, Izquierdo R, Ma DL (2011) Controlled fabrication of PbS

quantum-dot/carbon-nanotube nanoarchitecture and its significant contribution to near-infrared photon-to-current conversion. Adv Funct Mater 21:4010–4018

12. Lee JM, Kwon BH, Park HI, Kim H, Kim MG, Park JS, Kim ES, Yoo SH, Jeon DY, Kim SO (2013) Exciton dissociation and charge-transport enhancement in organic solar cells with quantum-dot/N-doped CNT hybrid nanomaterials. Adv Mater 25:2011–2017

13. Ma PC, Siddiqui AN, Maromb G, Kim JK (2010) Dispersion and functionalization of carbon nanotubes for polymer-based nanocomposites: a review. Compos Part A 41:1345–1367

14. Pornsunthorntawee O, Chuaybumrung S, Kitiyanan B, Chavadej S (2011) Purification of single-walled carbon nanotubes (SWNTs) by acid leaching, NaOH dissolution, and froth flotation. Sep Sci Technol 46:2056–2065

15. Kuznetsova A, Popova I, Yates JT, Bronikowski MJ, Huffman CB, Liu J, Smalley RE, Hwu HH, Chen JGG (2001) Oxygen-containing functional groups on single-wall carbon nanotubes: NEXAFS and vibrational spectroscopic studies. J Am Chem Soc 123:10699–10704

16. Cho N, Choudhury KP, Thapa RB, Sahoo Y, Ohulchanskyy T, Cartwright AN, Lee KS, Prasad PN (2007) Efficient photodetection at IR wavelengths by incorporation of PbSe-carbon-nanotube conjugates in a polymeric nanocomposite. Adv Mater 19:232–236

17. Klem EJD, Gregory CW, Cunningham GB, Hall S, Temple DS, Lewis JS (2012) Planar PbS quantum dot/C-60 heterojunction photovoltaic devices with 5.2% power conversion efficiency. Appl Phys Lett 100:173109

18. Jeong S, Shim HC, Kim S, Han CS (2010) Efficient electron transfer in functional assemblies of pyridine-modified NQDs on SWNTs. ACS Nano 4:324–330

19. Johnston KW, Pattantyus-Abraham AG, Clifford JP, Myskog SH, MacNeil DD, Levina L, Sargent EH (2008) Schottky-quantum dot photovoltaics for efficient infrared power conversion. Appl Phys Lett 92:151115

20. Law M, Luther JM, Song Q, Perkins CL, Nozik AJ (2008) Structural, optical, and electrical properties of PbSe nanocrystal solids treated thermally or with simple amines. J Am Chem Soc 130:5974–5985

21. Zheng SZ, Deng XY, Wong KY (2012) Enhancement of the power conversion efficiency of P3HT:PCBM based solar cells by an interfacial effect between P3HT and PEDOT. Synth Met 162:1490–1495

22. Mallajosyula AT, Sundar KIS, Baquer M (2010) Role of single walled carbon nanotubes in improving the efficiency of poly-(3-hexylthiophene) based organic solar cells. J Appl Phys 108:094902–094909

23. Stylianakis MM, Kymakis E (2012) Efficiency enhancement of organic photovoltaics by addition of carbon nanotubes into both active and hole transport layer. Appl Phys Lett 100:093301–093305

24. Fogden S, Howard CA, Heenan RK, Skipper NT, Shaffer MSP (2012) Scalable method for the reductive dissolution, purification, and separation of single-walled carbon nanotubes. ACS Nano 6:54–62

25. Kim HJ, Karim MR, Lee CJ, Doh WH (2012) Synthesis and characterization of a poly[(3-hexylthiophene-co-3-octylthiophene)]-SWNT composite for solar cell applications. J Nanoelectron Optoelectron 7:466–470

26. Filho SAG, Jorio A, Dresselhaus G, Dresselhaus MS, Saito R, Swan AK, Unlu MS, Goldberg BB, Hafner JH, Lieber CM, Pimenta MA (2002) Effect of quantized electronic states on the dispersive Raman features in individual single-wall carbon nanotubes. Phys Rev B 65:0354046

27. Gazi HAR, Guchhait B, Daschakraborty S, Biswas R (2011) Fluorescence dynamics in supercooled (acetamide plus calcium nitrate) molten mixtures. Chem Phys Lett 501:358–363

28. Guchhait B, Gazi HAR, Kashyap HK, Biswas R (2010) Fluorescence spectroscopic studies of (acetamide plus sodium/potassium thiocyanates) molten mixtures: composition and temperature dependence. J Phys Chem B 114:5066–5081

29. Olek M, Bulsgen T, Hilgendorff M, Giersig M (2006) Quantum dot modified multiwall carbon nanotubes. J Phys Chem B 110:12901–12904

30. Dabbousi BO, Rodriguez-Viejo J, Mikulec FV, Heine JR, Mattoussi H, Ober R, Jensen KF, Bawendi MG (1997) (CdSe)ZnS core–shell quantum dots: synthesis and characterization of a size series of highly luminescent nanocrystallites. J Phys Chem B 101:9463–9475

31. Efros AL, Rosen M (2000) The electronic structure of semiconductor nanocrystals. Annu Rev Mater Sci 30:475–521